Available online at www.sciencedirect.com
ScienceDirect
Journal of Photochemistry and Photobiology A: Chemistry 195 (2008) 116–126
Journal of Photochemistry and Photobiology A:Chemistry
www.elsevier.com/locate/jphotochem

Collective proton motion in the intramolecular hydrogen bonding network and the consequent enhancement in the acidity of hydroxycalixarenes

Mhejabeen Shaikh [a], Jyotirmayee Mohanty [a,*], Dilip K. Maity [b], Sandip K. Nayak [c], Haridas Pal [a,*]

[a] *Radiation & Photochemistry Division, Bhabha Atomic Research Centre, Trombay, Mumbai 400085, India*
[b] *Theoretical Chemistry Section, Bhabha Atomic Research Centre, Trombay, Mumbai 400085, India*
[c] *Bio-Organic Division, Bhabha Atomic Research Centre, Trombay, Mumbai 400085, India*

Received 30 May 2007; received in revised form 14 August 2007; accepted 25 September 2007
Available online 29 September 2007

Abstract

Interactions of two hydroxycalixarenes (HOCXs) and their alternate methoxy derivatives (MOCXs) with different proton acceptors (PA) like urea (U; pK_b = 13.9), *N*-methylurea (MU; pK_b = 13.1), and triethylamine (TEA; pK_b = 3.19) have been investigated using absorption and fluorescence measurements, to understand the role of intramolecular hydrogen bonding on the acidity of HOCXs and MOCXs. Both HOCXs and MOCXs show no interaction in their ground states with weak PAs like U and MU. In the excited (S_1) state, HOCXs interact, though moderately, with U and MU, involving hydrogen-bonded HOCX–U/MU exciplex formation. Excited MOCXs, however, do not show any interaction with U and MU. With TEA, a strong PA, the HOCXs show very strong interaction even in the ground state, though no interaction is observed for MOCXs. In the excited (S_1) state, the interaction in the HOCX–TEA system could not be resolved due to large static quenching arising via HOCX–TEA ground state complex formation. In the excited (S_1) state, MOCXs interact reasonably strongly with TEA, via the formation of hydrogen-bonded exciplexes. All these results are apparently in accordance with the pK_a values of the HOCXs and MOCXs, as estimated or judged from the pH dependent spectrophotometric measurements. Supportive evidence for the hydrogen bonded complex formation in these systems has been obtained from quantum chemical calculations. It is indicated from the present results that even though the phenolic OH groups in both HOCXs and MOCXs are intramolecularly hydrogen bonded, and thus expected to be less labile for deprotonation under normal circumstances than in normal phenol, the HOCXs show unusually higher acidity than expected. It is inferred that a collective proton motion in the intramolecular hydrogen bonding network in HOCXs causes an enhanced polarizability of the phenolic protons and consecutively the acidity of these molecules. In MOCXs, since no such collective proton motion is possible, they behave quite normally and display much weaker acidity than HOCXs and normal phenol.

Keywords: Calixarene; Proton acceptors; Hydrogen bonding; Collective proton motion; Exciplex

1. Introduction

Calixarenes and their derivatives are interesting class of molecules of having large intramolecular cavities suitable to encapsulate many guest molecules via supramolecular bindings [1–6]. In hydroxycalixarenes (HOCX) the intramolecular cavities are the result of alternate arrangements of phenolic and methylenic units in a cyclic manner and the presence of cyclic intramolecular hydrogen bonding network among all the phenolic OH groups. Depending on the number of phenolic units, homologues of different sizes are known, most prominent among them are tetra-HOCX, hexa-HOCX, and octa-HOCX. Calixarenes are not only structurally rigid but also chemically quite stable [1–6]. These calixarene based receptors form stable host–guest complexes and show high selectivity for many organic guest molecules and metal cations, and are reported to have a large number of potential applications in different areas [5–16]. Another interest in calixarenes is due to their structural

* Corresponding authors. Tel.: +91 22 2559 5396; fax: +91 22 2550 5151/2551 9613.
E-mail addresses: jyotim@barc.gov.in (J. Mohanty), hpal@barc.gov.in (H. Pal).

1010-6030/$ – see front matter © 2007 Elsevier B.V. All rights reserved.
doi:10.1016/j.jphotochem.2007.09.013

features mimicing some natural systems, e.g. *heme* mimics [17]. Presence of phenolic chromophores in calixarenes can serve as an intrinsic probe to investigate many of their properties and interactions by photochemical techniques, especially by monitoring their fluorescence emission [18,19]. Studies on the excited states of phenolic compounds including calixarenes can also provide many useful information on the fundamental processes like electron transfer (ET) reactions, hydrogen bonding interactions, proton transfer (PT) processes, etc. [18–24].

Although the guest binding properties of calixarene in solution are being studied intensively, using NMR spectroscopy, calorimetry, and UV–vis absorption spectroscopy, relatively little is known on the photochemical properties of the calixarenes [7,8,11,15,25]. By using the UV and ^{1}H NMR spectral studies, earlier Gutsche et al. have investigated the interaction of calixarenes with amines in acetonitrile (ACN) solution suggesting the interaction to involve a two step process, viz., proton transfer followed by complex formation [25]. Recently we have investigated the photoinduced ET interactions of some calixarene molecules with different chloroalkane (CA) acceptors [18,19] and the results have been compared with those obtained for chemically similar biphenol–CA systems [20]. Interestingly it was observed that unlike in biphenol–CA systems, where the interaction mainly occurs via a concerted dissociative ET (DET) mechanism, in calixarene–CA systems, the reaction proceeds by the combination of the stepwise and the concerted DET mechanisms, the former is due to the encaged CA acceptors and the latter is due to the free CA acceptors. In calixarenes, along with the cage effect, the phenolic OH groups can also participate in some specific interaction to recognize some selective guests. In this regard, some efforts have also been made in the literature to suitably modify the phenolic OH groups in calixarenes to enhance their effectiveness in some specific applications [26–28]. Since the phenolic OH groups in HOCXs are involved in the formation of cyclic intramolecular hydrogen bonding network [29–32], it is interesting to know and understand how these phenolic OH groups behave in terms of their acidity in comparison to other phenolic molecules. Herein we report the interactions of two HOCXs and their alternate methoxy derivatives (MOCX) with different proton acceptors (PA) using absorption and fluorescence measurement techniques to understand the effect of intramolecular hydrogen bonding present in these molecules on their binding and acidic characteristics. We also carry out quantum chemical calculations for the present systems to obtain supportive evidence for the inferences drawn from the observed photochemical studies. The two HOCXs studied are 5,11,17,23-tetra-*tert*-butyl-25,26,27,28-tetrahydroxy-calix[4]arene and 5,11,17,23,29,35-hexa-*tert*-butyl-37,38,39,40,41,42-hexahydroxy-calix[6]arene, and are abbreviated as tetra-HOCX and hexa-HOCX, respectively. The two MOCXs investigated in the present work are 5,11,17,23-tetra-*tert*-butyl-25,27-dimethoxy-26,28-dihydroxy-calix[4]arene and 5,11,17,23,29,35-hexa-*tert*-butyl-37,39,41-trimethoxy-38,40,42-trihydroxy-calix[6]arene, and are abbreviated as di-MOCX and tri-MOCX, respectively. The PAs used in the present study are urea (U; $pK_b = 13.9$, [33]) and *N*-methylurea (MU; $pK_b = 13.1$, [34]) as the weak PAs and triethylamine (TEA; $pK_b = 3.19$, [33]) as a strong PA. Chemical structures of HOCXs, MOCXs and PAs used in the present study are shown in Chart 1.

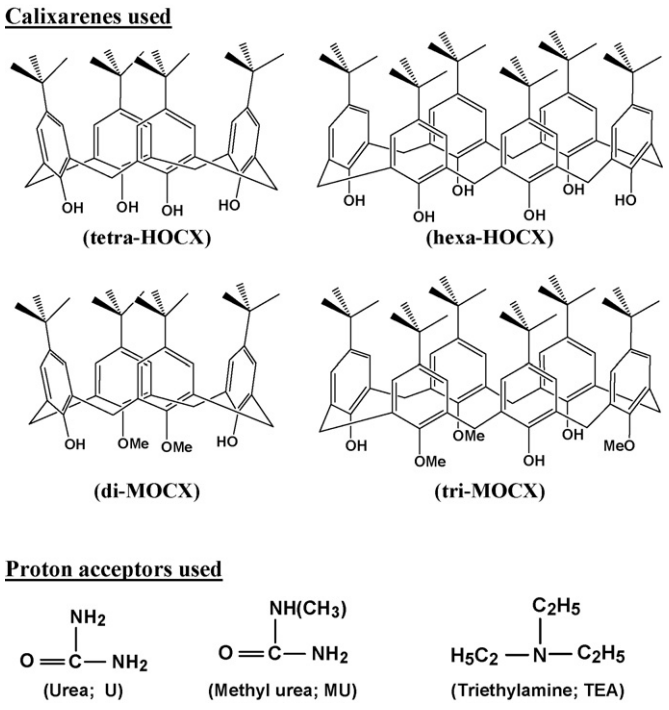

Chart 1.

2. Materials and methods

Tetra-HOCX and hexa-HOCX were obtained from Aldrich Chemical Co., USA, and used as received. Di-MOCX and tri-MOCX were synthesized following procedures reported in the literature [35,36]. The samples were purified by repeated crystallization from chloroform and fully characterized by IR, ^{1}H NMR and ^{13}C NMR data (*cf.* supporting information). GR grade U and MU were obtained from Fluka and used without further purification. TEA was obtained from Spectrochem, India, and purified by distillation just before use. Spectroscopic grade organic solvents were used in the present work and obtained from Spectrochem, India.

The absorption spectra of the samples were recorded in a Shimadzu model 160-A UV–vis spectrophotometer using 1 cm path length Suprasil quartz absorption cells. Steady-state (SS) fluorescence spectra were recorded in a Hitachi model F-4010 spectrofluorimeter using 1 cm × 1 cm Suprasil quartz cuvettes. All fluorescence spectra were recorded with corrections for the wavelength dependent instrument responses. Time-resolved (TR) fluorescence measurements were carried out using a time-correlated-single-photon-counting (TCSPC) spectrometer (Edinburgh Instruments, UK, model 199), described elsewhere [37]. Briefly, a thyratron-triggered, gated hydrogen discharge lamp, operating at a repetition rate of 30 kHz, was used as the excitation source and a Philips XP-2020Q PMT was used to detect the fluorescence photons. Observed fluorescence decays were analyzed using a reconvolution procedure [38]. The instru-

ment response functions (IRF) required for the reconvolution analyses were obtained independently by replacing the sample cell with a light scatter (TiO_2 suspension in water). Typical width of the IRF was about 1.2 ns (FWHM). The shortest lifetime measurable using the present setup following reconvolution analysis is about 0.2 ns. The observed fluorescence decays for the present systems were seen to fit well with a single-exponential function as [38],

$$I(t) = B \exp\left(-\frac{t}{\tau}\right) \quad (1)$$

where B is the pre-exponential factor and τ is the fluorescence lifetime of the sample. For all the fits, the χ^2 values were within 1.00–1.20 and the weighted residuals were randomly distributed among the data channels [38]. In the present study, all the measurements were carried out at ambient temperature ($25 \pm 1\,^{\circ}C$). For both steady-state and time-resolved measurements the HOCX and MOCX concentrations were kept reasonably low, only in the range of about 20–30 μM.

3. Results and discussion

3.1. Ground state interactions of HOCXs and MOCXs with different proton acceptors

In the presence of TEA, a strong PA ($pK_b = 3.19$), the absorption spectra of the two HOCXs in acetonitrile (ACN) solutions show a large change, causing a decrease in the absorbance of the 279 nm band due to that of HOCXs and the development of a new absorption band with peak at ~289 nm and shoulder at ~313 nm due to the formation of a new species. A clear isosbestic point at ~283 nm is also indicated. Typical of these results are shown in Fig. 1A for tetra-HOCX–TEA system. It is evident from Fig. 1A that the interaction of the HOCXs with TEA is very strong such that the spectral conversion of ~20 μM solution of HOCXs becomes almost complete with only ~400 μM of TEA. Since the phenolic OH groups in HOCXs can participate either in proton transfer (PT) or in hydrogen bonding (HB) interactions, the spectral changes in the present systems can either be due to the formation of the ionic species, $^{-}$OCX and $TEAH^+$, or due to the formation of the intermolecular HB-complexes like TEA···HOCX.

Considering a PT equilibrium in the HOCX–TEA systems, the changes in absorbance (A) at a wavelength where only the newly formed species absorbs (e.g. 313 nm) can be correlated as,

$$A \approx \frac{K\{[\mathrm{HOCX}]_0 + [\mathrm{TEA}]_0\} \pm \sqrt{K^2\{[\mathrm{HOCX}]_0 + [\mathrm{TEA}]_0\}^2 - 4(K-1)K[\mathrm{HOCX}]_0[\mathrm{TEA}]_0}}{2(K-1)}\varepsilon \quad (2)$$

where K is the equilibrium constant, ε is the molar extinction coefficient for the species at the measuring wavelength and $[HOCX]_0$ and $[TEA]_0$ are the total concentrations of HOCX and TEA used. Fig. 1B shows the plot of the changes in the absorbance at 313 nm for tetra-HOCX–TEA system with the TEA concentration. A fit of the data in Fig. 1B was deduced using Eq. (2) and is also shown by the dashed curve. The K values thus obtained for the two HOCX–TEA systems are of the order of 0.2. However, from the fitted curves following Eq. (2), it is evident that the fits are not that good for both the HOCX–TEA systems. It is thus indicated that the interaction in the HOCX–TEA systems might not be due to a PT reaction but could be due to the formation of the ground state TEA···HOCX complexes. Thus, we also tried to fit the experimental data on the basis of such HB-complex formation equilibrium, whereby the changes in the absorbance at the absorption band of the newly formed species were correlated using the following relation.

$$A = \frac{\{K([\mathrm{HOCX}]_0 + [\mathrm{TEA}]_0) + 1\} \pm \sqrt{\{K([\mathrm{HOCX}]_0 + [\mathrm{TEA}]_0) + 1\}^2 - 4K^2[\mathrm{HOCX}]_0[\mathrm{TEA}]_0}}{2K}\varepsilon \quad (3)$$

The fit of the data at 310 nm for tetra-HOCX–TEA system following Eq. (3) is shown by the solid curve in Fig. 1B. It is evident that the fits thus obtained following Eq. (3) are far more superior than those obtained using Eq. (2). These results thus support the HB-complex formation in the present systems. The K values thus obtained for the two HOCX–TEA systems following Eq. (3) are of the order of $2.2 \times 10^4\ M^{-1}$, which are substantially high values, suggesting very strong hydrogen bonding interaction in the present systems. Similar complex formation between the calixarenes and amines has also been suggested by Gutsche et al. and the order of the K values match very well with the reported association constant values for HOCX-*tert*-butylamine/neopentylamine systems [25].

Unlike HOCXs, their methoxy derivatives, namely, di-MOCX and tri-MOCX (*cf.* Chart 1), are seen not to display any spectral change even in the presence of substantially high concentration (~0.3 M) of TEA. Thus it is indicated that MOCXs do not interact with TEA. In the present context it is interesting to compare present results with those obtained for normal phenol (ΦOH) in the presence of TEA. It is observed that like MOCXs, ΦOH also does not interact in its ground state with TEA. It is evident from the results of HOCXs, MOCXs and ΦOH that the phenolic OH groups in HOCXs show unusually higher acidity than those in MOCXs and ΦOH.

In the literature, the pK_a values of few water-soluble calixarene derivatives (e.g. sulphonate or nitro derivatives) and of some water insoluble calixarenes in ACN by selective titration with bases have been reported [25,26,39]. It has been observed that the pK_a value of normal phenol in ACN is 26.6, whereas the pK_a values of calixarenes in ACN solutions are in the range of 15–19, which suggests that the calixarenes are more acidic than ΦOH [26], a result in consistence with our present observation in the presence of TEA. The HOCXs and MOCXs investigated in the present work are not sufficiently soluble in water. We thus made an effort to estimate their pK_a values following the pH

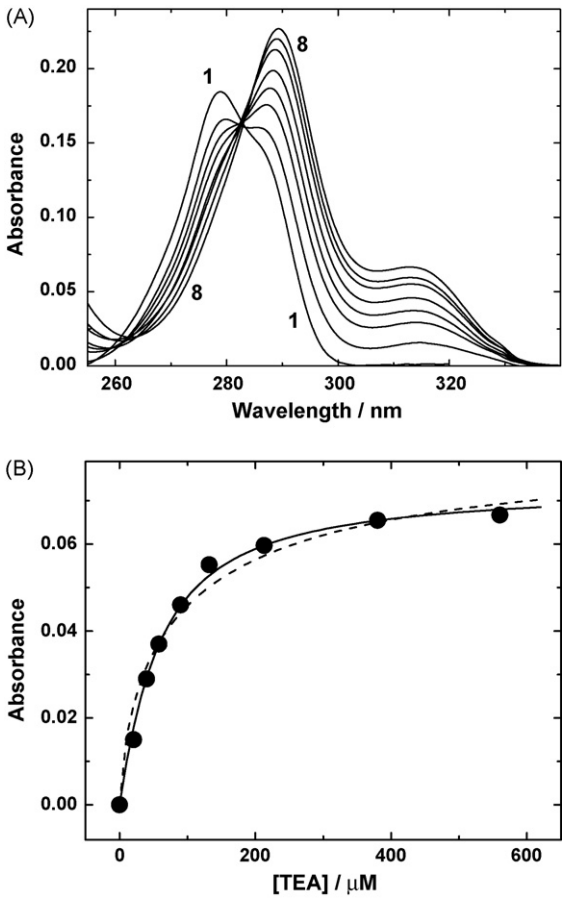

Fig. 1. (A) Absorption spectra of tetra-HOCX (19 μM) in ACN solution in the presence of different TEA concentrations. The spectra 1–8 correspond to 0, 21, 40, 58, 90, 132, 213 and 560 μM TEA, respectively. (B) Changes in the absorbance at 313 nm as a function of TEA concentration. The closed circles represent the experimental data. The dashed and solid curves represent the fits corresponding to Eqs. (2) and (3), respectively.

dependent changes in their absorption spectra in MeOH–water solvent mixture. About 40 volume percent of MeOH in water was needed to achieve the required solubility of the calixarenes in this study. We presume that the pH measurement in this solvent mixture is reasonable, as the water composition is still sufficiently high [40–43]. For both the HOCXs, following these measurements, their first pK_a values were estimated in the range of about 8.5. Though multiple pK_a values were expected for the HOCXs due to presence of more than one phenolic OH groups, in the present study we could not observe any other higher pK_a values, at least upto pH ∼ 12. Beyond pH ∼ 12, however, the measurements were not possible, as the solution became turbid at this high alkalinity.

Unlike HOCXs, the MOCXs do not show any pH dependent changes in their absorption spectra, at least up to pH ∼ 12. Thus, their first pK_a values must be higher than 12. For normal ΦOH, the pK_a value in water is reported to be about 10 [44]. In the present study, for a direct comparison with the calixarene systems, the pK_a value of ΦOH was also measured in 40% methanol solution. As expected, the pK_a value of ΦOH estimated in the present study is somewhat higher (pK_a = 10.4) than that reported in aqueous solution. Comparing the pK_a values of the calixarenes with ΦOH in 40% methanol solution it is clearly indicated that the HOCXs are much stronger acid than ΦOH but the MOCXs are much weaker acid than ΦOH. These results are in accordance with the results obtained on the ground state interactions of HOCXs and MOCXs with TEA. That MOCXs are weaker acid than ΦOH can easily be rationalized considering that the phenolic OH groups are intramolecularly hydrogen bonded with the adjacent OMe groups. Due to these hydrogen bondings, the phenolic protons in MOCXs become less labile for deprotonation than in normal ΦOH. Since all the phenolic OH groups in HOCXs are also expected to involve in a cyclic intramolecular hydrogen bonding network among themselves [29–32] the observation that the HOCXs show stronger acidity than ΦOH is quite surprising. This point will be discussed further in Section 3.2, where we present the results on the excited state (S_1) interactions of HOCXs and MOCXs with different PAs. In the present context, however, it was interesting to know how the HOCXs and MOCXs interact in their ground states with weak proton acceptors like U (pK_b = 13.9) and MU (pK_b = 13.1). To investigate this, absorption spectra of HOCXs and MOCXs (*cf.* Chart 1) were recorded in both acetonitrile (ACN) and methanol (MeOH) solutions in the presence of varying U and MU concentrations. In the present study, along with ACN we also use MeOH as a solvent, because the solubility of U/MU is much higher in the latter solvent (>2 M) than in the former (∼0.3 M). In either of the solvents, however, no changes were observed in the absorption spectra of HOCXs and MOCXs in the presence of U and MU. It is thus indicated that in the ground state both HOCXs and MOCXs do not interact with the weak PAs like U and MU.

3.2. Excited singlet (S_1) state interactions of HOCXs and MOCXs with proton acceptors

3.2.1. Interactions of HOCXs and MOCXs with weak proton acceptors, U and MU

The fluorescence intensity of HOCXs in MeOH solution is seen to undergo significant quenching in the presence of U and MU. In ACN solution, though quenching is certainly indicated, yet the extent of quenching is not sufficiently large, even at the solubility limit of U/MU (∼0.3 M). Thus, in the present study, we mainly used MeOH as the solvent where solubility of U/MU is very high (>2 M) and accordingly substantial quenching can be observed. It is seen that the fluorescence band of HOCXs at ∼305 nm undergoes a significant quenching in the presence of U/MU. A longer wavelength new emission band (∼440 nm) with extremely low intensity also develops in these systems as the U/MU concentration is increased in the solution. Fig. 2A shows the typical steady-state (SS) fluorescence results for tetra-HOCX–U system in MeOH solution. Present results indicate that the HOCXs interact quite significantly in their excited singlet (S_1) state with U and MU. As the acidity of phenolic molecules increases in the S_1 state [44], quenching of HOCXs fluorescence by weak PAs like U/MU can be possible, even though in the ground state HOCXs do not interact with these PAs. The weak new emission band that develops at ∼400 nm is certainly due to an excited species photogenerated during the

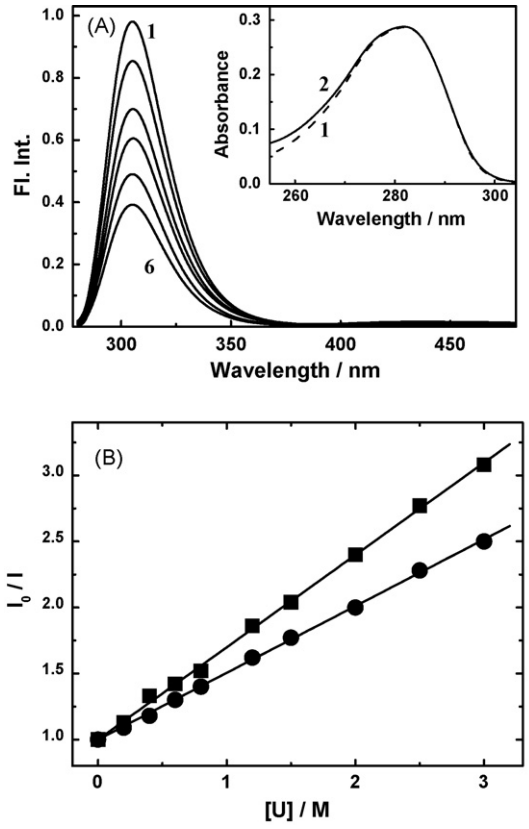

Fig. 2. (A) Fluorescence spectra of tetra-HOCX (29 μM) in MeOH solution in the presence of different U concentrations. Spectra 1–6 correspond to 0, 0.4, 0.8, 1.2, 2.0 and 3.0 M U, respectively. Inset: Absorption spectra of tetra-HOCX in methanol: (1) in absence and (2) in presence of 3.0 M U. (B) The I_0/I vs. [U] plots for tetra-HOCX–U (■) and hexa-HOCX–U (●) systems in MeOH solution. The plots are linear as expected from SV relation.

interaction, as no interaction was observed in the ground state of the HOCXs.

Unlike HOCXs, both MOCXs and ΦOH do not show any interaction in their excited states with U and MU. For ΦOH in aqueous solution, its excited (S_1) state acid dissociation constant (pK_a^*) is 5.7, about 4.3 units lower than the ground state pK_a [44]. Considering a similar extent of reduction in the pK_a^* value in 40% MeOH solution, the expected pK_a^* value for ΦOH in 40% MeOH solution should be ~6.1. On the basis of the same consideration, the pK_a^* values of HOCXs in 40% MeOH solutions are expected to be in the range of ~4.2 and those of MOCXs are expected to be >7.7. Thus, the S_1 states of HOCXs are expected to be much more acidic than that of ΦOH and accordingly can show interactions even with the weak PAs like U and MU.

The SS fluorescence quenching of HOCXs by U and MU in MeOH solution were correlated using Stern–Volmer (SV) relation as [44,45],

$$\frac{I_0}{I} = 1 + K_{SV}[PA] = 1 + k_q\tau_0[PA] \quad (4)$$

where I_0 and I are the fluorescence intensities (at 305 nm) in the absence and presence of PAs, respectively, τ_0 is the fluorescence lifetime of HOCXs in the absence of PAs (*cf.* Table 1), K_{SV} is the Stern–Volmer constant and k_q is the bimolecular quenching constant. Typical I_0/I versus [PA] plots for two HOCX–U systems are shown in Fig. 2B. The k_q values obtained for different HOCX–U/MU systems are listed in Table 1. It is seen that the k_q values for the HOCX–U/MU systems are only of the order of $(2–3) \times 10^8\ M^{-1}\ s^{-1}$, about two orders of magnitude lower than the typical bimolecular diffusion-controlled rate constant, $k_d \sim 2 \times 10^{10}\ M^{-1}\ s^{-1}$ [45]. Thus, the interaction in the present systems is indicated to be only moderate in nature. Since the pK_a^* values of HOCXs are only about 1.9 unit lower than that of ΦOH, such a moderate interaction for the excited HOCXs with U and MU might be quite reasonable, considering that the excited state of ΦOH does not even interact with U/MU.

To get more insight of the interaction mechanism in the HOCX–U/MU systems, we measured the fluorescence lifetimes (τ) of the HOCXs in the presence of varying U/MU concentrations. In all these cases, the fluorescence decays (at 305 nm) are seen to fit well with a single-exponential function. Typical of these decays and their single exponential analyses are shown in Fig. 3. It is seen that the τ values of the HOCXs gradually decrease on increasing U/MU concentration, suggesting a dynamic nature of interaction between excited HOCXs and ground state U/MU. In the interaction mechanism, if no exciplex type of intermediates were forming, the reduction in the τ values with U/MU concentrations were expected to follow a linear SV relation as [44,45],

$$\frac{\tau_0}{\tau} = 1 + k_q\tau_0[PA] \quad (5)$$

where τ_0 and τ are the fluorescence lifetimes in the absence and presence of the quenchers. For the present systems, however, the τ_0/τ versus [PA] plots are seen to show a downward curvature instead of following the SV linearity. Typical of these results are shown in Fig. 4A. Present observation indicates that the interaction in these systems involves the formation of exciplexes (EX)

Table 1
Kinetic parameters for different calixarene–PA systems obtained from SS and TR fluorescence quenching studies

Calixarenes	Solvents	τ_0 (ns)	PA	k_q ($10^8\ M^{-1}\ s^{-1}$)	K_{eq} (M^{-1})	k_p ($10^9\ s^{-1}$)
tetra-HOCX	MeOH	2.50	U	2.80	0.19	2.4
hexa-HOCX	MeOH	2.26		2.24	0.21	1.2
tetra-HOCX	MeOH	2.50	MU	2.94	0.3	1.5
hexa-HOCX	MeOH	2.26		2.36	0.21	1.3
di-MOCX	ACN	2.32	TEA	5.38	3.03	0.63
tri-MOCX	ACN	2.79		6.46	3.03	0.62

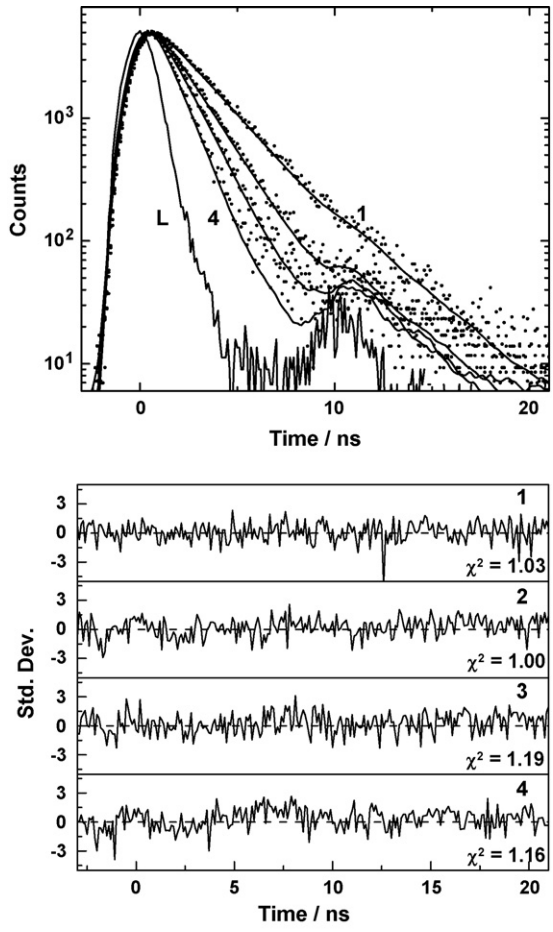

Fig. 3. Fluorescence decays for tetra-HOCX (29 μM) in MeOH solution measured at 305 nm with excitation at 280 nm in the presence of different U concentrations. Curves 1–4 correspond to 0, 0.5, 1.0 and 2.0 M U, respectively. Experimental decays are shown by dotted curves. Single exponential fits to the decays are shown by solid curves. The curve L represents the instrument response function. The fitting parameters are: (1) $\tau = 2.42$ ns, $\chi^2 = 1.03$; (2) $\tau = 1.7$ ns, $\chi^2 = 1.0$, (3) $\tau = 1.15$ ns, $\chi^2 = 1.19$ and (4) $\tau = 0.98$ ns, $\chi^2 = 1.16$. The lower panel of the figure shows the distribution of the weighted residuals among the data channels.

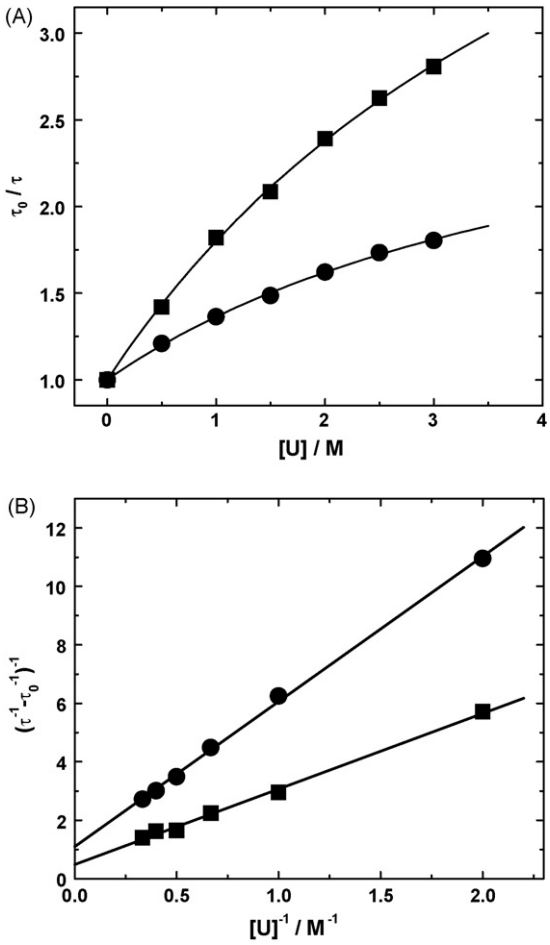

Fig. 4. (A) The τ_0/τ vs. [U] plots for tetra-HOCX–U (■) and hexa-HOCX–U (●) systems in MeOH solution. The plots show downward curvature from SV linearity. Solid curves show the fit of the data following Eq. (10). (B) The $\{\tau^{-1} - \tau_0^{-1}\}^{-1}$ vs. $[U]^{-1}$ plots for tetra-HOCX–U (■) and hexa-HOCX–U (●) systems in MeOH solution. The plots are linear as expected from Eq. (11).

as the intermediates [45–49]. Thus, the interaction in the present systems can be presented by the following Scheme 1 [45,46], where k_f and k_{nr} are the fluorescence and nonradiative rate constants for excited HOCXs ($k_f + k_{nr} = \tau_0^{-1}$), k_1 and k_2 are the formation and dissociation rate constants of the exciplex and k_p is the deexcitation rate constant of the exciplex.

Following Scheme 1, SS fluorescence quenching should correlate with the U/MU concentrations as [45,46],

$$\frac{I_0}{I} = 1 + \frac{k_1 k_p \tau_0 [PA]}{k_2 + k_p} \tag{6}$$

As suggested by this equation, the I_0/I versus [PA] plots should follow a SV type of linearity, as observed for the HOCX–U/MU systems. Regarding TR measurements, on the basis of Scheme 1, the fluorescence decays of HOCXs should in general be expressed as [45,46],

$$I(t) = C_1 \exp\left(\frac{-t}{\tau_1}\right) + C_2 \exp\left(\frac{-t}{\tau_2}\right) \tag{8}$$

where the lifetimes τ_1 and τ_2 and the pre-exponential factors C_1, and C_2 are the functions of k_1, k_2, k_f, k_{nr}, k_p and the PA concentration used. Thus, a bi-exponential fluorescence decay of HOCXs was normally expected in the presence of U/MU. However, under some circumstances, especially when the exciplex equilibrium is established very quickly in comparison to the fluorescence decay time of HOCXs, observed decay could

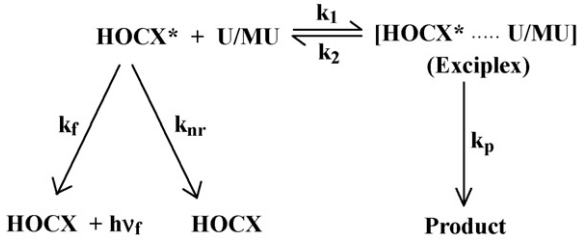

Scheme 1.

effectively fit with a single-exponential function [45,46]. In these cases, the observed fluorescence lifetime can be expressed as,

$$\tau = \frac{1 + K_{ex}[PA]}{\tau_0^{-1} + K_{ex}k_p[PA]} \quad (9)$$

where $K_{ex} = k_1/k_2$ is the equilibrium constant of the exciplex formation. Rearranging Eq. (9) we can express the τ_0/τ ratio as,

$$\frac{\tau_0}{\tau} = \frac{1 + K_{ex}k_p\tau_0[PA]}{1 + K_{ex}[PA]} \quad (10)$$

It is evident from Eq. (10) that the τ_0/τ versus [PA] plot for these systems should show a downward curvature instead of following the SV linearity. For the present systems, we tried to fit the experimental TR data following Eq. (10). Typical of such fits for HOCX–U systems are shown in Fig. 4A with the continuous curves. The K_{ex} and k_p values thus estimated for different HOCX–U/MU systems are listed in Table 1. We also analyzed the TR data for the HOCX–U/MU systems using a linear form of expression (9) as [46,47],

$$\{\tau^{-1} - \tau_0^{-1}\}^{-1} = \{K^{-1}(k_p - \tau_0^{-1})^{-1}\}[PA]^{-1} + \{(k_p - \tau_0^{-1})\} \quad (11)$$

Typical $\{\tau^{-1} - \tau_0^{-1}\}^{-1}$ versus $[PA]^{-1}$ plots for HOCX–U/MU systems are shown in Fig. 4B. As expected, these plots are linear within experimental error. From the slopes and intercepts of these plots, the K_{ex} and k_p values were also estimated for different HOCX–U/MU systems and are found to be similar to those obtained from the direct fits of the data using Eq. (10).

3.2.2. Interactions of HOCXs and MOCXs with strong proton acceptor, TEA

As already shown in Section 3.1, both tetra-HOCXs and hexa-HOCXs interact very efficiently in their ground states with the strong proton acceptor TEA. To understand the effect of TEA on the fluorescence characteristics of HOCXs, SS fluorescence measurements were carried out in ACN solution exciting the samples at 283 nm (isosbestic point). It is seen that the fluorescence intensity of HOCXs at ~309 nm undergoes a drastic reduction even in the presence of only few hundred μM of TEA concentration. Concomitant to this quenching, an extremely weak new fluorescence band at ~420 nm is also seen to develop, very similar to that observed in the HOCX–U/MU systems. Typical of these results are shown in Fig. 5. In a solvent like ACN, the maximum diffusion-controlled bimolecular rate constant k_d is expected to be in the range of $\sim 2 \times 10^{10}\ M^{-1}\ s^{-1}$ [44,45]. For the present systems, if the quenching constant k_q is even considered to be similar to that of k_d, the effective pseudo-first order quenching constant $k_q[PA]$ in the presence about 500 μM of TEA is estimated to be only $\sim 1 \times 10^7\ s^{-1}$. On the contrary, the self-decay rate constants ($k_f + k_{nr} = \tau_0^{-1}$, τ_0 is the fluorescence lifetime in the absence of TEA) for the excited HOCXs are of the order of

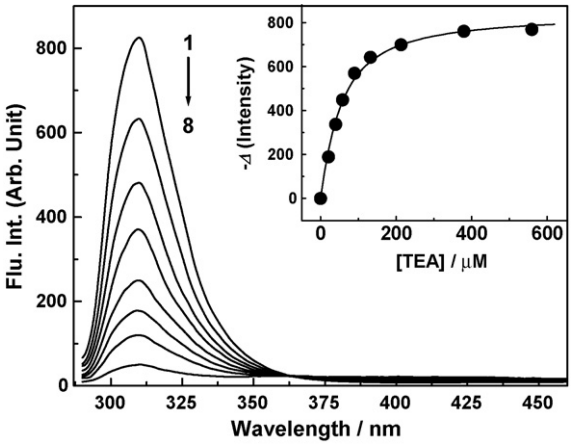

Fig. 5. Fluorescence spectra of tetra-HOCX (19 μM) in ACN solution in the presence of different TEA concentrations. Spectra 1–8 correspond to 0, 21, 40, 58, 90, 132, 213 and 560 μM TEA. Inset: Plot of the changes in the fluorescence intensity against the TEA concentration. Solid circles are the experimental data points and the solid curve is the fit of the data following Eqs. (12) and (13).

$\sim 4 \times 10^8\ s^{-1}$. It is thus evident that the fluorescence quenching observed for the two HOCXs in the presence of few hundred μM of TEA concentration must be due to the strong static-quenching arising due to the ground state TEA···HOCX complex formation, rather than any dynamic interaction of TEA with the excited HOCX molecules. Thus, for the HOCX–TEA systems, observed fluorescence quenching was simply considered as the static quenching and accordingly the change in the fluorescence intensity at 309 nm was correlated using the following relation [50,51],

$$\Delta I = \left(\frac{[HOCX]_{eq}}{[HOCX]_0} - 1\right) I^0_{Dye} \quad (12)$$

where $[HOCX]_0$ is the total HOCX concentration used, $[HOCX]_{eq}$ is the free HOCX in the solution in equilibrium with the TEA···HOCX complex and I^0_{Dye} is the observed fluorescence intensity in the absence of TEA. The $[HOCX]_{eq}$ values at each TEA concentration used were estimated as,

$$[HOCX]_{eq} = \frac{\{K[HOCX]_0 - K[TEA]_0 - 1\} + \sqrt{\{K[HOCX]_0 + K[TEA]_0 + 1\}^2 - 4K^2[HOCX]_0[TEA]_0}}{2K} \quad (13)$$

where $[HOCX]_0$ and $[TEA]_0$ are the total HOCX and TEA concentrations used, respectively, and K is the equilibrium constant for the TEA···HOCX complex formation. Inset of Fig. 5 shows the ΔI versus [TEA] plot for tetra-HOCX–TEA system along with the fitted curve obtained following Eqs. (12) and (13). It is seen that the fit is very satisfactory. The K values thus estimated for the two HOCX–TEA systems are of the order of $2.5 \times 10^4\ M^{-1}$, which are quite similar to the values estimated from the absorption studies (*cf.* Section 3.1). These results thus support our inference that the SS fluorescence quenching in HOCX–TEA systems is mainly due to static quenching arising due to the ground state TEA···HOCX complex formation. This is further supported from the observation that the SV type of I_0/I versus [TEA] plots (not shown in the figures) for the HOCX–TEA systems show a gradual upward curvature, indicat-

ing the effect of ground state complex formation [44,45]. Since the effect of ground state complex formation is very large in the present systems, it was not possible to separate out the excited state interaction parameters for the HOCX–TEA systems from the fluorescence quenching measurements. For the present systems, we also carried out the TR fluorescence measurements to see the effect of TEA on the τ values of HOCXs. As expected, no observable change was noticed in the τ values with about 500 μM concentration of TEA. At much higher TEA concentrations, the TR measurements were not possible due to very weak fluorescence from these systems.

With MOCXs, though there was no ground state interaction with TEA, in the S_1 state the MOCXs showed reasonable interaction with TEA, as evident from SS fluorescence quenching studies. Typical SS fluorescence results for tetra-MOCX–TEA system in ACN are shown in Fig. 6A. It is evident from these results that the MOCX–TEA systems behave quite similar to the HOCX–U/MU systems. It is seen that the SS quenching of the MOCXs fluorescence (at ~312 nm) by TEA follows a linear SV-relationship. Typical I_0/I versus [TEA] plots for MOCX–TEA systems are shown in Fig. 6B. The k_q values obtained for different MOCX–TEA systems are listed in Table 1. Like HOCX–U/MU systems, the k_q values in MOCX–TEA systems are also quite lower in comparison to the typical diffusion-controlled bimolecular rate constant ($\sim 2 \times 10^{10}\ M^{-1}\ s^{-1}$), suggesting the interaction is also moderate for the present systems. This is in fact expected considering a much lower acidity of MOCXs in comparison to that of HOCXs.

From TR measurements, it is seen that the τ values of MOCXs decrease gradually on increasing the TEA concentration in the solution. The τ_0/τ versus [TEA] plots for these systems are seen to undergo a downward curvature than the SV linearity, as also observed for HOCX–U/MU systems. Typical τ_0/τ versus [PA] plots for MOCX–TEA systems are shown in Fig. 7A. It is evident from these results that like in HOCX–U/MU systems, in MOCX–TEA systems also the excited state interaction follows via the hydrogen bonded exciplex formation (*cf.* Scheme 1). Accordingly the τ_0/τ versus [PA] plots for MOCX–TEA systems were analyzed following Eq. (10). The K_{ex} and k_p values thus estimated for the present systems are listed in Table 1. The lifetime data for these systems were also analyzed following Eq. (11), whereby linear $\{\tau^{-1} - \tau_0^{-1}\}^{-1}$ versus $[TEA]^{-1}$ plots were obtained as shown in Fig. 7B. The K_{eq} and k_p values thus

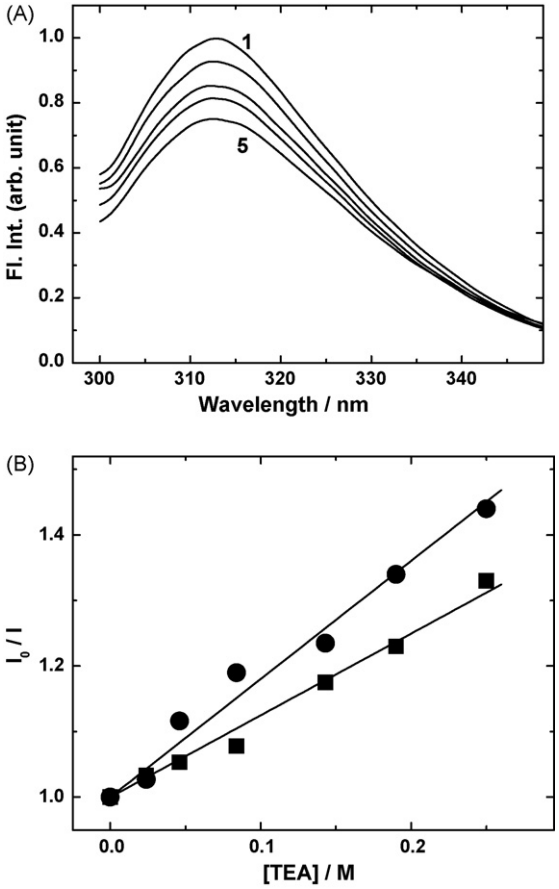

Fig. 6. (A) Fluorescence spectra of di-MOCX (19 μM) in ACN solution in the presence of different TEA concentrations: spectra 1–5 correspond to 0, 0.08, 0.14, 0.19 and 0.25 M [TEA]. (B) The I_0/I vs. [TEA] plot for di-MOCX–TEA (■) and tri-MOCX–TEA (●) systems in acetonitrile solutions. The plots are linear within experimental error.

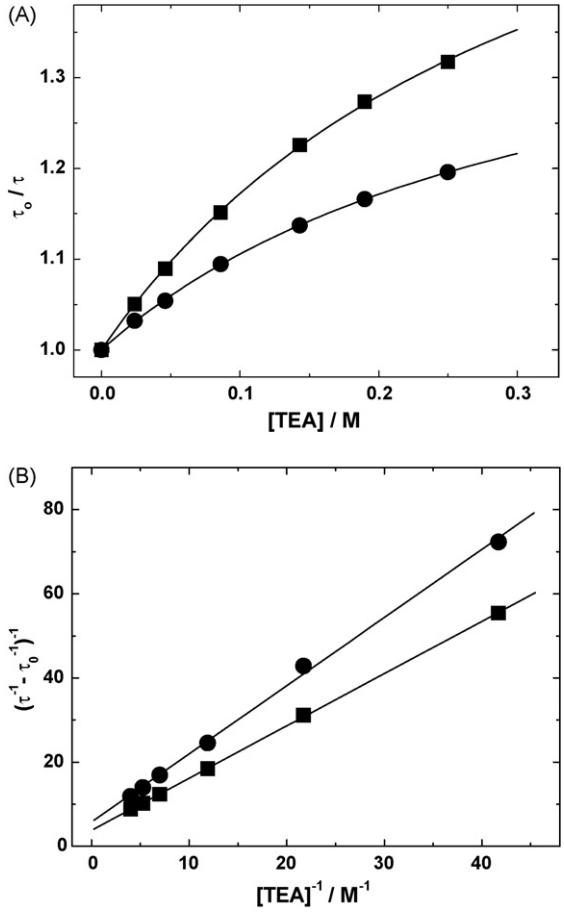

Fig. 7. (A) The τ_0/τ vs. [TEA] plots for di-MOCX–TEA (●) and tri-MOCX–TEA (■) systems in acetonitrile solutions. The plots show negative deviation from SV linearity. Solid curves show the fit of the data following Eq. (10). (B) The $\{\tau^{-1} - \tau_0^{-1}\}^{-1}$ vs. $[TEA]^{-1}$ plots for di-MOCX–TEA (●) and tri-MOCX–TEA (■) systems in acetonitrile solutions. The plots are linear as expected from Eq. (11).

obtained from the slopes and intercepts of these plots are similar to those obtained from the direct fitting of the data following Eq. (10).

Comparing all the results for different HOCX–PA and MOCX–PA systems, it is evident that the phenolic OH groups in HOCXs are much more acidic than those in MOCXs and ΦOH. Since all the phenolic OH groups in HOCXs are expected to be engaged in a cyclic intramolecular hydrogen bonding network among themselves [29–32], it was expected under normal circumstances that the phenolic OH groups in HOCXs should be less labile for deprotonation than that in ΦOH. A similar situation is also expected for the phenolic OH groups in MOCXs because of the involvement of the OH groups in intramolecular hydrogen bonding interaction with the adjacent OMe groups. Accordingly, the phenolic OH groups in MOCXs are less labile for deprotonation, causing their pK_a values to increase by more than about 2 units than that of ΦOH. A simple consideration of the intramolecular hydrogen bonding effect in HOCXs is, however, unable to account the enhanced acidity in HOCXs. It is evident that the phenolic protons in HOCXs are much more polarizable than those in MOCXs, even though the formers are also involved in intramolecular hydrogen bonding. We presume that the cyclic intramolecular hydrogen bonding network present in HOCXs causes a special effect in these molecules to make the phenolic protons to undergo a collective motion in the cyclic hydrogen bonding network and thereby increasing their polarizability. To be mentioned here that the roll of collective proton motion to enhance proton polarizability has also been suggested by Brzezinski and co-workers [29,52] for a number of chemical systems having intramolecular hydrogen bonding network. As shown by these authors, even in the anionic forms of such systems, the negative charge can attain an extra stabilization due to the delocalization of the charge via the collective proton motion in the hydrogen bonding network. Since a collective proton motion is highly feasible in HOCXs, these molecules show much higher acidity than even ΦOH. Since a similar collective proton motion is not possible in MOCXs, their acidity is much weaker than that of HOCXs and ΦOH. In fact, in MOCXs, the presence of localized hydrogen bonding involving phenolic OH groups and adjacent OMe groups causes their phenolic protons to be less labile for deportation. In HOCXs, as the collective proton motion is possible, we predict that in HOCX–PA systems either the ground state complex or the exciplex is formed due to the simultaneous interaction of all the phenolic protons with the PA, as schematically shown in Scheme 2. In MOCXs, the interaction with PA like TEA to form exciplex is possibly due to localized hydrogen bonding interaction, involving one of the phenolic protons of MOCXs, as collective proton motion is not possible in MOCXs. In brief, we suggest that, due to the presence of collective proton motion in the intramolecular hydrogen bonding network, HOCXs show unusually higher acidity than MOCXs and ΦOH.

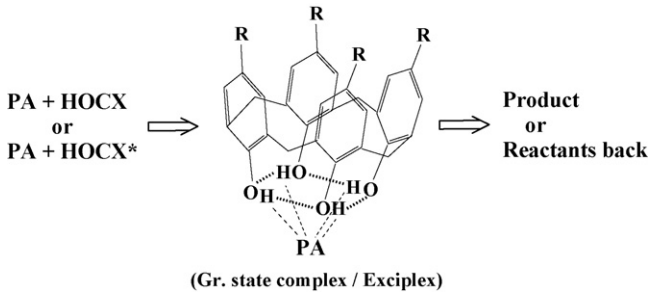

Scheme 2.

To support the formation of hydrogen bonded complex between HOCXs and PAs, as shown in Scheme 2, quantum chemical calculations were carried out for some of the selective systems, namely HOCX–TEA systems. As the present calixarene-PA systems are very large, the geometry optimization of calixarenes was carried out at semiempirical AM1 level of theory [53]. Geometry optimization of TEA was also carried out at the same level and the optimized TEA structure was placed out side the calixarene rim containing the phenolic OH groups with the amino nitrogen of TEA orienting towards phenolic OH groups of HOCXs such that the H-bonded TEA···HOCX complexes can be formed. The whole system was then optimized at AM1 level and the final energy minimized structures thus obtained for the tetra- and hexa-HOCX–TEA systems are shown in Fig. 8. The optimized structures of these systems indicate, at

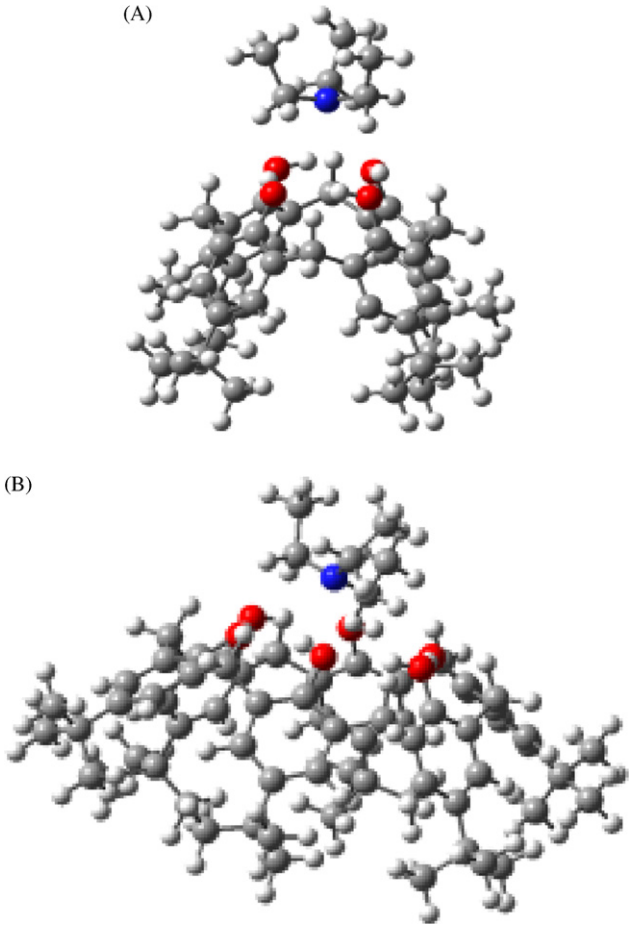

Fig. 8. The energy minimized structures of (A) tetra-HOCX–TEA and (B) hexa-HOCX–TEA systems, as obtained from AM1 level of quantum chemical calculations, are shown the figure. The structures qualitatively indicate the intermolecular hydrogen bonded complex formation between TEA and HOCX molecules.

least qualitatively, the formation of intermolecular H-bonded complexes. In these structures shown in Fig. 8, the distances between amino nitrogen of TEA and all the hydroxyl hydrogen atoms of tetra-HOCX are calculated to be in the range of about 2.7–2.9 Å. For hexa-HOCX–TEA systems, however, the distances between amino nitrogen of TEA and hydroxyl hydrogen atoms of HOCX are predicted to be in two different ranges, one set (two H) is in the range of 3.1–3.4 Å and the other set (four H) is in the range of 4.0–4.1 Å. For the tetra- and hexa-HOCX–TEA systems, the binding energies for the complexes are calculated to be about 5.2 and 5.8 kcal/mol, respectively. It is to mention here that in case of tetra-HOCX–TEA system, even when the TEA was placed with a different orientation with respect to the HOCX in the initial guess structure such that the intermolecular hydrogen bonding is not possible to start with, successive energy minimization leads to the same final structure as shown in Fig. 8A. Similar AM1 calculations were also carried out for di- and tri-MOCX–TEA systems. It is observed that the final energy minimized structures of these two systems largely depend on the orientation of amino nitrogen of TEA with respect to the MOCX in the initial guess structures. When the initial guess structure was such that amino nitrogen of TEA was orientated towards the OH groups of MOCXs, then the distances between amino nitrogen of TEA and the hydroxyl hydrogen atoms of MOCXs are much larger (>1.0 Å) for both di- and tri-MOCX–TEA systems in comparison to the tetra- and hexa-HOCX–TEA systems. The binding energies are also calculated to be about 2.2 and 2.7 kcal/mol less for the di- and tri-MOCX–TEA systems, respectively, compared to the tetra- and hexa-HOCX–TEA systems. These results suggest a much weaker intermolecular interaction in MOCX–TEA systems in comparison to that in HOCX–TEA systems and thus qualitatively support the experimental results where HOCXs is seen to undergo very strong interaction with TEA but MOCXs effectively do not show any observable interaction with TEA, at least in the ground state. To verify the observed AM1 results, calculations were also carried out at the density functional theory (DFT) level applying B3LYP correlated hybrid functional and split valence Gaussian basis function 6–31G(d,p) [54] with the AM1 optimized structure for tetra-HOCX–TEA system. Incidentally, the binding energy for the system is calculated to be ∼5.0 kcal/mol, very similar to that obtained from AM1 calculation. The geometry of the tetra-HOCX–TEA complex was further optimized at B3LYP/6–31G(d,p) level. Though the calculation was rather difficult with such a large system, the optimized structure was observed to be very similar to that of the AM1 optimized structure. Thus, geometry optimization for the remaining systems were not carried out at the DFT level. In the present study all the quantum chemical calculations were carried out following GAMESS program system [55].

Finally, it is to be mentioned that in solution phase some of the calixarene derivatives can undergo conformational changes, whereby the conformations other than the cone structures can also be possible, in which one or more phenolic OH groups can remain detached or isolated from the intramolecular hydrogen bonding network. These isolated phenolic OH groups can thus undergo easier deprotonation than the ones involved in intramolecular hydrogen bonding. For the HOCXs and MOCXs studied, the above conformational changes seem to be quite unlikely, due to the steric effect of the bulky tertiary butyl groups in the *para* positions. It is thus expected that the present HOCX and MOCX molecules will mainly exist in their cone conformation, where the OH/OMe groups are in the same side of the calixarene ring, facilitating the intramolecular hydrogen bond formation [1–6]. Moreover, in HOCXs, if the enhanced acidity was due to the presence of some free OH groups, the acidity was expected to be at the most similar to that of ΦOH. Moreover, since similar conformations with free OH groups should also have been possible for MOCXs, their acidity should have been quite similar to that of HOCX. Since the acidity of MOCXs is much weaker than that of HOCXs and ΦOH, we predict that the enhanced acidity in HOCXs is due to the higher polarizability of the phenolic protons, as arises due to the collective proton motion in the cyclic intramolecular hydrogen bonding network in the HOCX molecules.

4. Conclusions

Ground and excited (S_1) states of HOCXs and MOCXs are seen to interact at varying extents with different proton acceptors, like U, MU, and TEA. In the ground state, HOCXs do not show any interaction with weak proton acceptors like U and MU, but interact very strongly with stronger proton acceptor like TEA, forming ground state TEA···HOCX complexes. In the excited (S_1) state, HOCXs interact moderately with U and MU, via the formation of hydrogen bonded exciplexes. Though MOCXs do not interact in their ground state with any of the PAs used, in the S_1 state they interact with the strong PA like TEA via the formation of hydrogen bonded exciplexes as the intermediates. The ground state absorption and the SS and TR fluorescence results in the present systems have been correlated using suitable kinetic schemes for ground state complex and/or exciplex formation. Different kinetic and equilibrium parameters have also been estimated for these systems from the experimental results. A support for the intermolecular hydrogen bonded complex formation in the present systems has also been obtained from quantum chemical calculations. Comparing the experimental results of different HOCX/PA and MOCX/PA systems it has been indicated that the HOCXs show unusual enhancement in their acidity compared to that of MOCXs and ΦOH. Contrary to HOCXs, the MOCXs show significantly lower acidity, lower than even ΦOH. The results are rationalized on the basis of the nature of the intramolecular hydrogen bonding present in HOCX and MOCX molecules. It is understood that the lower acidity in MOCXs is due to the less tendency of deprotonation of their phenolic OH groups that are locally hydrogen bonded to the adjacent OMe groups. In HOCXs, it is predicted that the enhanced acidity arises due to the collective motion of the phenolic protons in the cyclic intramolecular hydrogen bonding network, whereby the phenolic protons become much more polarizable than in ΦOH and MOCXs. A simultaneous interaction of all the phenolic protons with the PAs seems to be the reason for the stronger interaction of the HOCXs with different PAs.

Acknowledgements

Authors are thankful to Dr. S.K. Sarkar, Head, RPCD, and Dr. S. Chattopadhyay, Head, BOD, for their constant support and encouragement.

Appendix A. Supplementary data

Supplementary data associated with this article can be found, in the online version, at doi:10.1016/j.jphotochem.2007.09.013.

References

[1] A. Ikeda, S. Shinkai, Chem. Rev. 97 (1997) 1713.
[2] C.D. Gutsche, Calixarenes, in: J.F. Stoddart (Ed.), Monographs in Supramolecular Chemistry, vol. 1, Royal Society of Chemistry, Cambridge, 1989.
[3] C.D. Gutsche, Calixarenes Revisited, Royal Society of Chemistry, Cambridge, 2002.
[4] T.A. Hanna, L. Liu, A.M. Angeles-Boza, X. Kou, C.D. Gutsche, K. Ejsmont, W.H. Watson, L.N. Zakharov, C.D. Incarvito, A.L. Rheingold, J. Am. Chem. Soc. 125 (2003) 6228.
[5] V. Böhmer, Angew. Chem. Int. Ed. Engl. 34 (1995) 713.
[6] S. Ibach, V. Prautzsch, F. Vögtle, C. Chartroux, K. Gloe, Acc. Chem. Res. 32 (1999) 729.
[7] A.F.D. Danil de Namor, O. Jafou, J. Phys. Chem. B 105 (2001) 8018.
[8] A. Casnati, S. Barboso, H. Rouquette, M.J. Schwing-Weill, F. Arnaud-Neu, J.F. Dozol, R. Ungaro, J. Am. Chem. Soc. 123 (2001) 12182.
[9] C. Lynam, K. Jennings, K. Nolan, P. Kane, M.A. McKervey, D. Diamond, Anal. Chem. 74 (2002) 59.
[10] T. Konishi, A. Ikeda, T. Kishida, B.S. Rasmussen, M. Fujitsuka, O. Ito, S. Shinkai, J. Phys. Chem. A 106 (2002) 10254.
[11] S. Bhattacharya, S.K. Nayak, S. Chattopadhyay, M. Banerjee, A.K. Mukherjee, J. Phys. Chem. B 107 (2003) 11830.
[12] A.F.D. Danil de Namor, S. Chahine, E.E. Castellano, O.E. Piro, J. Phys. Chem. B 108 (2004) 11384.
[13] J.M. Notestein, A. Katz, E. Iglesia, Langmuir 22 (2006) 4004.
[14] R. Zadmard, T. Schrader, J. Am. Chem. Soc. 127 (2005) 904.
[15] Y. Liu, B.-H. Han, Y.-T. Chen, J. Phys. Chem. B 106 (2002) 4678.
[16] S. Mizyed, P.E. Georghiou, M. Ashram, J. Chem. Soc. Perkin Trans. 2 (2000) 27.
[17] C.D. Gutsche, K.C. Nam, J. Am. Chem. Soc. 110 (1988) 6153.
[18] J. Mohanty, H. Pal, S.K. Nayak, S. Chattopadhyay, A.V. Sapre, J. Chem. Phys. 117 (2002) 10744.
[19] J. Mohanty, H. Pal, S.K. Nayak, S. Chattopadhyay, A.V. Sapre, Chem. Phys. Lett. 370 (2003) 641.
[20] J. Mohanty, H. Pal, A.V. Sapre, J. Chem. Phys. 116 (2002) 8006.
[21] L.M. Tolbert, J.E. Haubrich, J. Am. Chem. Soc. 116 (1994) 10593.
[22] D. Huppert, E. Kolodney, M. Gutman, E. Nachliel, J. Am. Chem. Soc. 104 (1982) 6949.
[23] M.T. Htun, A. Suwaiyan, A. Baig, U.K.A. Klein, J. Phys. Chem. A 102 (1998) 8230.
[24] M.T. Htun, A. Suwaiyan, U.K.A. Klein, Chem. Phys. Lett. 243 (1995) 71.
[25] C.D. Gutsche, M. Iqbal, I. Alam, J. Am. Chem. Soc. 109 (1987) 4314.
[26] I.D. Cunningham, M. Woolfall, J. Org. Chem. 70 (2005) 9248.
[27] P.R.A. Webber, G.Z. Chen, M.G.B. Drew, P.B. Beer, Angew. Chem., Int. Ed. 40 (2001) 2265.
[28] G. Tumcharern, T. Tuntulani, S.J. Coles, M.B. Hursthouse, J.D. Kilburn, Org. Lett. 5 (2003) 4971.
[29] B. Brzezinski, H. Urjasz, G. Zundel, J. Phys. Chem. 100 (1996) 9021.
[30] D. Diamond, K. Nolan, Anal. Chem. 73 (2001) 22A.
[31] T. Grady, S.J. Harris, M.R. Smyth, D. Diamond, Anal. Chem. 68 (1996) 3775.
[32] T.V. Tolpekina, W.K. den Otter, W.J. Briels, J. Phys. Chem. B 107 (2003) 14476.
[33] D.R. Lide (Ed.), CRC Handbook of Chemistry and Physics., 80th ed., CRC Press, Boca Raton, 1999–2000.
[34] J.C. Penedo, M. Mosqvera, F. Rodriguez-Prieto, J. Phys. Chem. A 104 (2000) 7429.
[35] R.G. Janseen, W. Verboom, D.N. Reinhoudt, A. Casanatti, M. Freriks, A. Pochini, F. Ugozzoli, R. Ungaro, P.M. Nieto, M. Carramolino, F. Cuevas, P. Prados, J. de Mendoza, Synthesis (1993) 380.
[36] P.J. Dijkstra, J.A.J. Brunink, K.-E. Bugge, D.A. Reinhoudt, S. Harkema, R. Ungaro, F. Ugozzoli, E. Ghidini, J. Am. Chem. Soc. 111 (1989) 7567.
[37] S. Nad, H. Pal, J. Chem. Phys. 116 (2002) 1658.
[38] D.V. O'Connor, D. Phillips, Time Correlated Single Photon Counting, Academic Press, New York, 1984.
[39] U. Lünig, Adv. Phys. Org. Chem. 30 (1995) 63.
[40] H. Pal, T. Mukherjee, J.P. Mittal, J. Chem. Soc. Faraday Trans. 90 (1994) 711.
[41] T. Mukherjee, A.J. Swallow, P.M. Guyan, J.M. Bruce, J. Chem. Soc. Faraday Trans. 86 (1990) 1483.
[42] C.C. Westcott, pH Measurements, Academic Press, New York, 1978.
[43] R.L. Willson, Chem. Commun. (1971) 1249.
[44] K.K. Rohatgi Mukherjee, Fundamentals of Photochemistry, Wiley Eastern Limited, New Delhi, India, 1992.
[45] J.B. Birks, Photophysics of Aromatic Molecules, Wiley-Intersience, New York, 1970.
[46] W.R. Ware, W. Watt, J.D. Holmes, J. Am. Chem. Soc. 96 (1974) 7853.
[47] V.N. Grosso, C.A. Chesta, C.M. Previtali, J. Photochem. Photobiol. A: Chem. 118 (1998) 157.
[48] S.D. Choudhury, S. Basu, Chem. Phys. Lett. 373 (2003) 67.
[49] M.C. Rath, H. Pal, T. Mukherjee, J. Phys. Chem. A 105 (2001) 7945.
[50] J. Mohanty, A.C. Bhasikuttan, W.M. Nau, H. Pal, J. Phys. Chem. B 110 (2006) 7945.
[51] W.M. Nau, X. Zhang, J. Am. Chem. Soc. 121 (1999) 8022.
[52] B. Brzezinski, P. Radziejewski, J. Olejnik, G. Zundel, J. Phys. Chem. 97 (1993) 6590.
[53] M.J.S. Dewar, E.G. Zoebisch, E.F. Healy, J.P.P. Stewart, J. Am. Chem. Soc. 107 (1985) 3902.
[54] A.D. Beeke, J. Chem. Phys. 98 (1993) 5648.
[55] M.W. Schmidt, K.K. Baldridge, J.A. Boatz, S.T. Elbert, M.S. Gordon, J.H. Jensen, S. Koseki, N. Matsunaga, K.A. Nguyen, S.J. Su, T.L. Windus, M. Dupuis, J.A. Montgomery, J. Comput. Chem. 14 (1993) 1347.